Functionalized magnetic nanoparticles for efficient enrichment and sensitive detection of low abundant protein biomarker

R. Y. Capangpangan,[a] M. A. C. dela Rosa,[b,c] R. P. Obena,[d] Y.J. Chou,[e] D.L. Tzou,[d] S.J. Shih,[e] M.H. Chiang,[d] C.C. Lin,[f] and Y.J. Chen[b,d]

Caraga State University, Ampayon Butuan City, Philippines; Department of Chemistry, National Taiwan University, Taiwan; Nanoscience and Technology, Taiwan International Graduate Program; Institute of Chemistry, Academia Sinica Taiwan; Material Science and Engineering, National Taiwan University of Science and Technology; Department of Chemistry, National Tsing Hua University, Taiwan;
reycapangpangan@gmail.com

Abstract

In this work, we have developed a streamlined protocol for the synthesis and biological implementation of monodisperse magnetic nanoparticles that includes (a) fabrication of core MNPs using thermal decomposition, (b) surface protection by gold coating (MNP@Au) and surfactant coating using (MNP@IGEPAL) and lastly, (c) oriented functionalization of antibodies to maximize immuno-affinity.

On the model study of C-reactive protein (CRP), a serum biomarker for inflammatory process and cardiovascular diseases, the MNP dispersibility and size uniformity augments sensitive detection of low abundant disease biomarkers in a human serum sample. Compared to aggregated magnetic nanoparticles synthesized from the conventional co-precipitation method (MNP_{CP}), the detection sensitivity for CRP at extremely low amount of serum sample (1 μL) was enhanced ~19- and ~15-fold when monodisperse MNP@Au and MNP@IGEPAL, respectively, were used. In addition, the non-specific detection of abundant serum proteins were greatly reduced. Furthermore, this approach (1 ng/mL, S/N = 3) provided detection sensitivity of a 1000-fold lower concentration than the clinical cut-off (1 μg/mL) of CRP. Most interestingly, the enrichment efficiency correlates more closely with the MNP dispersibility than with the ligand density. Our study not only developed a simple and facile biofunctionalization protocol maintaining excellent solvent dispersibility, but also revealed the critical role of MNP dispersibility on immunoaffinity enrichment and detection of low abundant serum protein biomarker.

Introduction

In recent years, advances in nanotechnology have propelled forward and drawn significant attention to the production of different nanostructures particularly in biomedical applications, e.g. cancer detection. Nanotechnology can provide novel tools and complement existing ones in detecting biomarkers and provide successful strategies for real time and direct readout of genomic and proteomic information at the single molecule and single-cell level. Biomarkers, originally defined as measurable and quantifiable biological parameters which serve as indices for health- and physiology-related assessments, such as disease risk, psychiatric disorders, environmental exposure and its effects, disease diagnosis, metabolic processes, substance abuse, pregnancy, cell line development, epidemiologic studies, etc. As noted, identifying and detection of disease biomarkers in proteomics is too complicated, hence high throughput, sensitive, low-cost, fast, simple and accurate methods are desirable. In the proteomics era, mass spectrometry-based detection is an indispensable technique for biomarker detection and screening. Likewise, recent developments in mass spectrometry have greatly expanded the possibility of characterizing unknown proteins in proteomic research. Mass spectrometry is especially suitable for the direct detection of proteins (i.e., on the probe), which enhances specificity without the use of fluorescent or radioactive labels, offering greater flexibility in the selection of bioactive probes.

Due to their remarkable properties such as magnetic, biocompatibility and excellent surface functionality, magnetic nanoparticles, nanomaterials received considerable interest and are potentially useful in biomedicine and bioengineering, particularly in the detection of protein biomarkers. To achieve excellent performance in analyte-specific biochemical assays that are highly dependent on the physical characteristics of the nanoparticles, magnetic nanoparticle homogeneity, controllable size, large surface area, higher effective magnetic moment, longer decay time (slow sedimentation), and excellent solvent dispersity (non-aggregated) among other

properties are considered as critical factors. The analytical performance of nanoparticle-based methods for protein extraction (affinity probe) is inherently being compromised by nanoparticle aggregation, which in turn may significantly affect detection sensitivity towards the target analytes.

In this work, the interplay between nanoparticle homogeneity and dispersity in relation to disease biomarker enrichment and detection was studied. By far, this is the first attempt to provide quantitative correlation on the detection sensitivity with nanoparticle physical properties such as characteristic decay time and magnetic property (effective magnetic moment). It is hypothesized that the enrichment performance of a nanoprobe towards a certain analyte, in this case, a target protein antigen is influenced by dispersity and homogeneity of the nanoparticles. It is assumed that longer interaction time with the target analyte and ease of separation of nanoprobes are caused by synergism between nano-particle dispersity and magnetic property (effective magnetic moment) which in turn may significantly influence the enrichment efficiency of the nanoprobe. To demonstrate this, three kinds of magnetic nanoprobes from two different synthetic preparations of core nanoparticles were compared; monodisperse gold-coated magnetic nanoparticles (MNP@Au) and monodisperse IGEPAL-coated magnetic nanoparticles (MNP@IGEPAL) were prepared using thermal decomposition method while polydisperse MNP_{CP} was prepared from co-precipitation method.

Experimental

Synthesis of monodisperse magnetic nanoparticles by thermal decomposition method

A mixture composed of $Fe(acac)_3$ (0.71 g, 2 mmol) in phenyl ether (20 ml), oleic acid (2 ml, 6 mmol) and oleylamine (2 ml, 6 mmol) was stirred under nitrogen environment. 1,2-hexadecanediol (2.58 g, 10 mmol) was added and the mixture heated to reflux (200°C) for 30 min and then further heated under reflux (265C) for another 30 min. The obtained nanoparticles (cooled at room temperature) were precipitated by adding ethanol (~40 ml) and separated by centrifugation for 10 min (~6000 rpm). Hexane was added to re-dissolve the obtained nanoparticle pellet after centrifugation in the presence of oleic acid (~0.05 ml) and oleylamine (~0.05 ml.) Centrifugation (6000 rpm, 10 min) was then carried out to remove the undispersed residues. The final MNP was then precipitated by adding ethanol, centrifuged (6000 rpm, 10 min) and re-dispersed into hexane and stored at 4C until needed.

Synthesis of gold-coated MNPs (MNP@Au)

A mixture composed of $Fe(acac)_3$ (0.71 g) in phenyl ether (20 ml), oleic acid (2 ml) and oleyl-amine (2 ml) was stirred under nitrogen environment. Addition of 1,2-hexadecanediol (2.58 g) was carried out and the mixture heated to reflux (210°C) for 2 hr. After cooling to room temperature, the phenyl ether reaction solution containing Fe_3O_4 was used without purification as seeds for the gold coating process. The nanoparticle mixture (10 ml, ~0.33 mmol Fe_3O_4) was mixed with $Au(OOCH_3)_3$ (0.83 g), 1,2-hexadecane-diol (3.1 g), oleic acid (0.5 ml), oleylamine (3 ml) and phenyl ether (30 ml) and was heated to 190C for 1.5 hours. The particles were washed with ethanol and re-dispersed in hexane (repeated twice). After washing with ethanol, the gold-coated magnetic nanoparticles were separated from non-magnetic gold nanoparticles using a magnet and the final pellet dispersed in hexane with ~75 mM oleic acid and oleylamine to produce MNP@Au.

Synthesis of NH_2-MNP@Au

An ethanolic solution of 2-aminoethanethiol (cysteamine hydrochloride) was prepared by dissolving 2-aminoethanethiol (200 mg) in 90% ethanol (6 ml). To this, MNP@Au (from *B*) (10 mg) dispersed in chloroform (5 ml) was added and was stirred for 2 hr. The nanoparticles were magnetically isolated and washed with 80% ethanol thrice. The final nanoparticles were dried in vacuum and stored until needed.

Synthesis of NH_2-MNP@IGEPAL

The crude phenyl ether Fe_3O_4 mixture obtained in (*A*) was purified by precipitating with ethanol (~20 ml) and isolated via centrifugation (6000 rpm, 10 min). The nanoparticle pellets were dispersed with hexane in the presence of oleic acid (0.05 ml) and oleylamine (0.05 ml) and subsequent centrifugation (6000 rpm, 10 min) was carried out to remove any undispersed residue. Then, an equivalent amount (1 mg) of dried nanoparticle was dispersed in cyclohexane (1 ml) and added to a previously sonicated (30 min) IGEPAL-cyclohexane mixture (1 mmol/10 ml cyclohexane). The mixture was stirred for 4 hours at room temperature. Then, NH_4OH (80 µl) and TEOS (60 µl) was sequentially added and the mixture was continuously stirred for 30 hr at room temperature. APS (50 µl) was added thereafter and stirring was continued for another 18 hr. The particles were then precipitated and washed with ethanol several times and then dried under vacuum until needed.

Fabrication of boronic acid-oriented antibody nanoprobe

Amine-functionalized magnetic nanoparticles (2 mg), DSS (10 mg) and DMSO (250 µl) were mixed and sonicated for 30 min with occasional shaking every 10 min. Vigorous vortexing for 30 min and incubation for 6 hr was carried out. The nanoparticle mixture was then washed with DMSO thrice. 3-amino-phenylboronic acid (200 µl, 50 mM) was then added and incubated for 12 hr at 4C. The supernatant was removed by magnetic separation before addition of ethanolamine (200 µl, 100 mM). The mixture was then further incubated for additional 6 hr at 4°C and washed with water five times. Then, 200 µg of antibody dissolved in 200 µl of PBS buffer (CRP and SAA) was added and was further incubated for 12 hr at 4C. The nanoparticles were then washed with PBS buffer three times followed by the addition of dextran (40 µl, 2.5 mg/ml) and incubation for 6 hr (@ 4°C). Washing with PBS was finally carried out and the nanoparticles were dispersed to a final concentration of 10 mg/ml.

Fabrication of protein G-oriented antibody nanoprobe

DSS (10 mg) and amine-functionalized magnetic nanoparticles (2 mg) were dispersed with DMSO (250 µl). The resulting mixture was sonicated for 30 min with occasional mixing every 10 min. Vigorous shaking under vortex was conducted for another 30 min and incubation at room temperature for 2 hr was carried out thereafter. After isolation with magnet, the nanoparticles were washed with DMSO thrice. Protein-G (5 µg/µl, 40 µl) was added to the resulting mixture and incubated for 1 hr at 4°C. A blocking agent, MEG (100 mM, 40 µl) was then added and incubated at 4°C for 12 hr. After separation with magnet, the particles were washed with PBS (pH 7.4) five times. Then, 200 µg of antibody dissolved in 200 µl of PBS buffer (AFP) was added and then incubated for an additional of 12 hr at 4°C. The antibody-nanoparticle conjugates were washed with PBS thrice and with TEOA (1000 µl, 0.2 M, pH = 8.2) twice. DMP in TEOA solution (6.5 mg DMP/1 ml TEOA) was then added and agitated for 45 min at room temperature. Washing with ethanolamine (1000 µl, 0.1 M, pH = 8.2) once and subsequent agitation for 1 hr at room temperature was carried out. The nanoparticles were finally washed with PBS buffer thrice and dispersed in the same buffer to make a final concentration of 10 mg/ml and kept at 4C until used.

Results and Discussion

Monodisperse Magnetic Nanoparticles

TEM analysis as shown in Fig. 1 revealed that narrow size distribution and non-aggregated nanoparticles were obtained with an average size of 7.75 ± 0.791 nm (CV = 10.2%) and 22.38 ± 1.245 nm (CV = 5.56%) for NH_2-MNP@Au (Fig. 1C) and NH_2-MNP@IGEPAL (Fig. 1B), respectively. By definition, monodisperse nanoparticles were defined as those with less than 5% CV and near-monodisperse as those with less than 15% CV. According to this criterion, both NH_2-MNP@Au and NH_2-MNP@IGEPAL appear to be near-monodisperse. Conversely, severe aggregation was observed for NH_2-MNP_{CP} (Fig. 1A), and hence the size distribution of the nanoparticle cannot be ascertained.

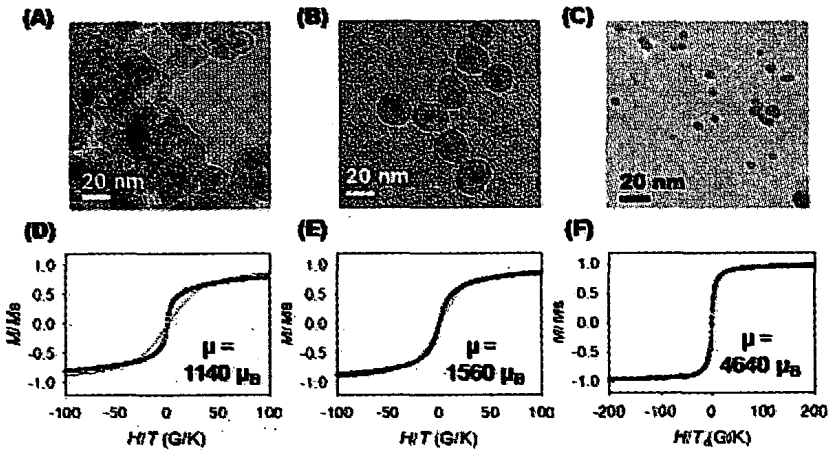

Fig. 1. Transmission electron microscope (TEM) images of (A) MNP_{CP}, (B) MNP@IGEPAL and (C) MNP@Au.

Decay time data reveal excellent dispersibility of MNP@Au and MNP@IGEPAL over conventional MNP_{CP}

The dispersibility of these nanoprobes was further evaluated by measuring the polydispersity index (PDI) from the Dynamic Light Scattering (DLS) experiment. As shown, the PDI values corroborated well with the TEM results, which is a measure of the nanoprobe dispersibility. NH_2-MNP@Au was observed to be near-monodisperse as it exhibited the lowest PDI value (0.096), followed by NH_2-MNP@IGEPAL (0.213) and lastly by NH_2-MNP_{CP} (0.537) with the highest PDI value. This result implies that the monodispersity of NH_2-MNP@Au and NH_2-MNP@IGEPAL over the conventional NH_2-MNP_{CP} will have a significant effect towards the target biological applications of these nanoprobes.

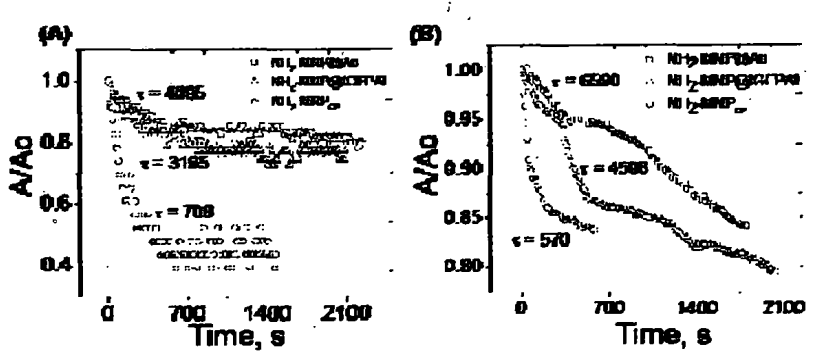

Fig. 2. Behavior of nanoparticles in (A) PBS buffer and (B) PBS-diluted serum determined by decay time.

Excellent dispersibility was observed for both NH_2-MNP@Au and NH_2-MNP@IGEPAL as compared with conventional NH_2-MNP_{CP} in both PBS buffer and in PBS-diluted serum solutions. Fig. 2A and 2B shows the decay curves for the nanoparticles dispersed in PBS and in PBS-diluted serum solution, respectively. As reflected in Fig, 2A, NH_2-MNP@Au showed ~6 fold longer decay time and NH_2-MNP@IGEPAL ~5 fold longer time than the NH_2-MNP_{CP}. This implies that NH_2-MNP@Au and NH_2-MNP@IGEPAL will take a longer time to start to settle because they formed a stable suspension, and hence have excellent dispersibility compared with NH_2-MNP_{CP}. In PBS-diluted serum, a similar trend was observed: NH_2-MNP@Au showed ~12 fold longer decay time and NH_2-MNP@IGEPAL ~8 fold longer time than NH_2-MNP_{CP}. These results indicate that NH_2-MNP_{CP} severely aggregates in serum and suggest that the dynamic instability of NH_2-MNP_{CP} suspensions in both PBS solution and in biological fluids caused particles to settle very fast compared with the other two nanoparticles. The stability of nanoparticle suspensions is reported to be regulated by inter-particle interactions, mainly van der Waals interactions, which stem from both the type of magnetic core and surface coatings.

Magnetic Nanoprobes for Immunoaffinity Enrichment and Detection of C-Reactive Protein

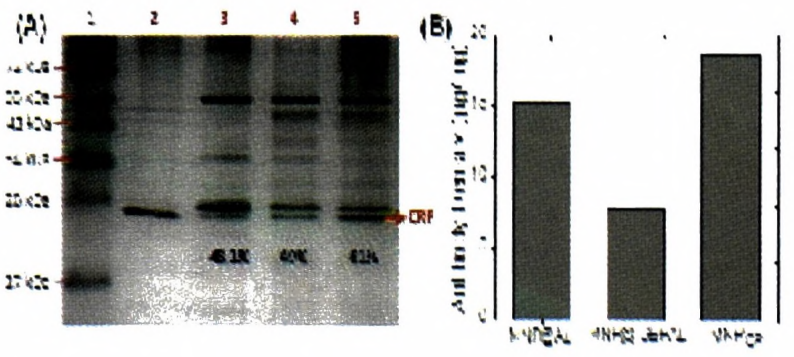

Fig. 3. (A) Recovery of Ab-MNPs by SDS-PAGE at saturating amounts of antigen. Lane 1: PAGE Ruler; Lane 2: CRP positive control, 500 ng; Lane 3: CRP 500 ng enriched by MNP_{CP}; Lane 4: CRP 500 ng enriched by MNP@IGEPAL; Lane 5: CRP 500 ng enriched by MNP@Au; (B) Antibody density of the different nanoprobes

The recoveries of the nanoparticles at high analyte concentration (1000 ng/mL) were first assessed to understand what the key factors that affect the enrichment performance are. Furthermore, to assess the performance of the core MNP material itself, we evaluated the recoveries (Fig. 3A) at the same amount of core MNP (20 µg) regardless of the amount of antibody conjugated to the nanoparticle (antibody density). MNP@Au has the highest recovery (61%), with MNP@IGEPAL (49%) and MNP_{CP} (48.1%), having similar recoveries. This trend does not correlate with the antibody densities of the nanoparticles (Fig. 3B). MNP@Au and MNP_{CP} have almost similar antibody densities (15.3 µg/mg Ab MNP and 18.4 µg/mg, respectively), while MNP@IGEPAL has the lowest antibody density (7.7 µg/mg). Theoretically, at high amounts of the antigen, the recovery would be mainly influenced by the antibody density. However, the lack in correlation demonstrates that other factors likely influence the enrichment performance.

As shown in Fig. 4A, a 6-fold signal enhancement was observed for MNP@Au and 5-fold for MNP@IGEPAL compared with MNP_{CP} at 10 µL serum. Moreover, in approximately "one drop of blood" (1 µL serum), CRP was enriched by both MNP@Au and MNP@IGEPAL, but not by MNP_{CP} (Fig. 4A). Considering that the concentration of CRP in serum of healthy individuals is 0.8-3 ng/µL[9], MNP@Au and MNP@IGEPAL are highly efficient to isolate nanogram levels of protein from a very complex mixture like serum, further demonstrating the dispersity effect.

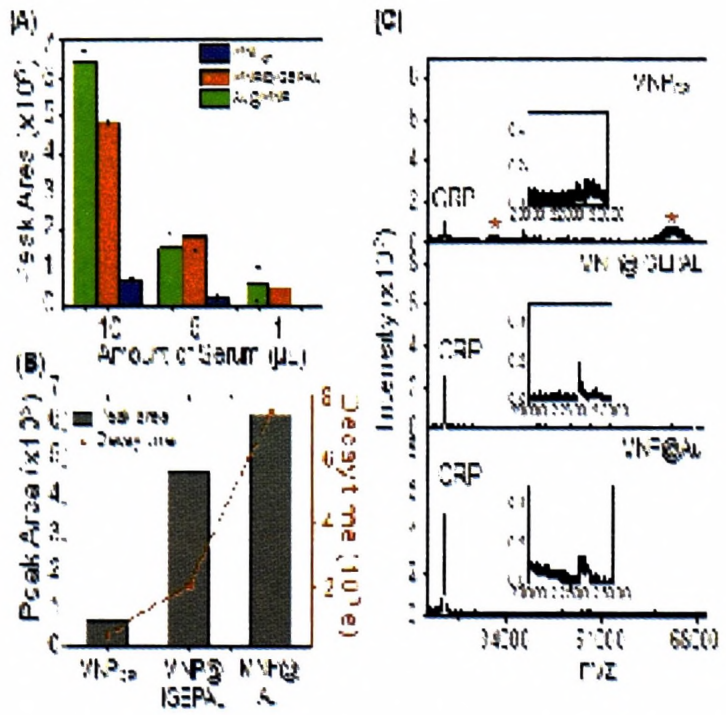

Fig. 4. Signal enhancement and reduction of non-specific binding from serum by well-dispersed nanoprobes. (A) CRP can be detected in as low as 1 µl serum by MNP@Au and MNP@IGEPAL. (B) Peak area increases proportionally with decay time in serum (10 µl). (C) MALDI spectra of CRP enriched from 10 µl unspiked diluted serum. Insets: Enrichment from "one drop" of blood: 1 µl unspiked serum. Serum was obtained from a healthy individual. All samples diluted with PBS.

As shown in Fig, 4B, the peak area increases with decay time, correlating the enrichment efficiency of the nanoparticle with its dispersibility. In an environment that contains minute analyte amount relative to the other components in solution, our nanoparticles have very good dispersibility hence are

able to stay longer in the solution, increasing the probability of capturing the target analyte. More importantly, the MALDI spectra, obtained between the range of 20-70 kDa, showed a marked reduction in non-specific binding with MNP@Au and MNP@IGEPAL (Figure 4C). Obviously, the reduced non-specific binding of MNP@Au and MNP@IGEPAL contributes to the sensitivity enhancement in serum. In PBS buffer, the performances of MNP@IGEPAL and MNP_{CP} were comparable. But the poor performance of MNP_{CP} in serum can be attributed to the non-specific binding of undesirable biomolecules on the nanoparticle, thus, lowering its efficiency[7]. Because of size uniformity and the relatively small size of MNP@Au and MNP@IGEPAL, the exposed surfaces of these nanoparticles were mostly covered by the larger antibody, which in turn may repel other non-specific proteins or biomolecules. This reduction in non-specific binding suggests that the advantages of nanoparticle dispersibility and size uniformity go beyond enhancement of detection sensitivity.

Conclusions

In summary, we have demonstrated a streamlined protocol based on thermal decomposition, gold and surfactant coating, and oriented antibody immobilization to fabricate monodisperse and stable immuno-MNPs in PBS buffer as well as in serum. We have also shown that the decay time of nanoparticles correlates well with their efficiencies in immunoaffinity enrichment of a disease biomarker protein. Of the three magnetic nanoparticles tested, MNP@Au demonstrated significant enhancement in sensitivity in both PBS buffer and human serum. More importantly, both MNP@Au and MNP@IGEPAL exhibited good sensitivity and specificity in diluted serum. The results may be attributed to the synergy between the dispersibility and size uniformity of nanoparticles. Well-dispersed magnetic nanoparticles provide a stable suspension which increases the probability of affinity-based extraction of target analyte, while size uniformity provides better specificity of nanoprobes to exclude non-specific extraction. With the demonstrated enhancement on enrichment sensitivity and specificity, we believe that well-dispersed nano-probes are promising materials not only for the detection and quantification of other disease biomarker from clinical specimens, but can also have other biomedical applications.

10. .

References

1. M. V. Yigit, A. Moore and Z. Medarova, *Pharmaceut. Res.* , 2012, **29**, 1180-1188.
2. A. S. Thakor and S. S. Gambhir, *CA: A Cancer J. Clinicians*, 2013, **63**, 395-418.
3. P. R. Srinivas, P. Barker and S. Srivastava, *Lab. Investigation*, 2002, **82**, 657-662.
4. R. S. Vasan, *Circulation*, 2006, **113**, 2335-2362.
5. P.-H. Chou, S.-H. Chen, H.-K. Liao, P.-C. Lin, G.-R. Her, A. C.-Y. Lai, J.-H. Chen, C.-C. Lin and Y.-J. Chen, *Analyt, Chem.*, 2005, **77**, 5990-5997.
6. P. H.-L. Tran, T. T.-D. Tran, T. Van Vo and B.-J. Lee, *Arch, Pharm. Res,* 2012, **35**, 2045-2061.
7. R. Y. Capangpangan, M. A. C. dela Rosa, R. P. Obena, Y.-J. Chou, D.-L. Tzou, S. J. Shih, M.-H. Chiang, C.-C. Lin and Y.-J. Chen, *Analyst*, 2015, **140**, 7678-7686.
8. M. Baalousha and J. R. Lead, *Nature Nanotech.,* 2013, **8**, 308-309.
9. M. B. Pepys and G. M. Hirschfield, *J. Clin. Investign.*, 2003, **111**, 1805